JOURNAL OF GEOPHYSICAL RESEARCH, VOL. 103, NO. A8, PAGES 17,205–17,213, AUGUST 1, 1998

Solar wind measurements with SOHO: The CELIAS/MTOF proton monitor

F. M. Ipavich,[1] A. B. Galvin,[1] S. E. Lasley,[1] J. A. Paquette,[1] S. Hefti,[2]
K.-U. Reiche,[3] M. A. Coplan,[1] G. Gloeckler,[1] P. Bochsler,[2]
D. Hovestadt,[4] H. Grünwaldt,[5] M. Hilchenbach,[5] F. Gliem,[3]
W. I. Axford,[5] H. Balsiger,[2] A. Bürgi,[4] J. Geiss,[2] K. C. Hsieh,[6] R. Kallenbach,[2]
B. Klecker,[4] M. A. Lee,[7] G. G. Managadze,[8] E. Marsch,[5] E. Möbius,[7]
M. Neugebauer,[9] M. Scholer,[4] M. I. Verigin,[8] B. Wilken,[5] and P. Wurz[2]

Abstract. The proton monitor, a small subsensor in the Charge, Element, and Isotope Analysis System/Mass Time-of-Flight (CELIAS/MTOF) experiment on the SOHO spacecraft, was designed to assist in the interpretation of measurements from the high mass resolution main MTOF sensor. In this paper we demonstrate that the proton monitor data may be used to generate reasonably accurate values of the solar wind proton bulk speed, density, thermal speed, and north/south flow direction. Correlation coefficients based on comparison with the solar wind measurements from the SWE instrument on the Wind spacecraft range from 0.87 to 0.99. On the basis of the initial 12 months of observations, we find that the proton momentum flux is almost invariant with respect to the bulk speed, confirming a previously published result. We present observations of two interplanetary shock events, and of an unusual solar wind density depletion. This large density depletion, and the correspondingly large drop in the solar wind ram pressure, may have been the cause of a nearly simultaneous large increase in the flux of relativistic magnetospheric electrons observed at geosynchronous altitudes by the GOES 9 spacecraft. Extending our data set with a 10-year time span from the OMNIWeb data set, we find an average frequency of about one large density depletion per year. The origin of these events is unclear; of the 10 events identified, 3 appear to be corotating and at least 2 are probably CME related. The rapidly available, comprehensive data coverage from SOHO allows the production of near-real time solar wind parameters that are now accessible on the World Wide Web.

1. Introduction

The Solar and Heliospheric Observatory (SOHO) mission is a joint venture of the European Space Agency and the U.S. National Aeronautics and Space Administration. The SOHO spacecraft was launched on December 2, 1995, and was inserted into a halo orbit about the L1 Sun-Earth Lagrangian point in February 1996. The scientific payload may be broadly classified into three main research areas: helioseismology, upper solar atmosphere remote sensing, and solar particle in situ measurements [*Domingo et al.*, 1995]. One of the solar particle experiments is the Charge, Element, and Isotope Analysis System (CELIAS) [*Hovestadt et al.*, 1995]. The CELIAS package includes two sensors devoted to solar wind composition studies (charge time of flight (CTOF) and mass time of flight (MTOF)) and one sensor devoted to solar wind proton measurements (the proton monitor (PM)). Because of its position at L1, far upstream of the Earth's magnetosphere and the Earth's foreshock region, the SOHO spacecraft samples solar wind that has not been modified by the presence of the Earth. The spacecraft is three-axis stabilized, always facing the Sun. Hence the SOHO mission provides a ideal platform with excellent collection power for nearly continuous, undisturbed solar wind studies. In addition, the typical solar wind at the SOHO L1 location, $\sim 1.5 \times 10^6$ km sunward of the Earth, is observed nearly 1 hour before it reaches the Earth, thus allowing an early warning of possible impending magnetospheric disturbances.

The proton monitor is a subsensor of the MTOF experiment. MTOF determines high-resolution mass spectra of heavy solar wind ions and uses a very wide bandwidth energy-per-charge analyzer to maximize counting statistics (at the expense of charge state information) for rare elements and isotopes. Since SOHO is not a spinning spacecraft, the deflection system was designed to have a wide angular acceptance in two dimensions. The PM was designed to assist in the interpretation of MTOF data and for that reason uses a similar wide bandwidth (and wide angular acceptance) analyzer that

[1]Department of Physics, University of Maryland, College Park.
[2]Physikalisches Institut der Universität, Bern, Switzerland.
[3]Institut für Datenverarbeitungsanlagen, Technische Universität, Braunschweig, Germany.
[4]Max-Planck-Institut für extraterrestriche Physik, Garching, Germany.
[5]Max-Planck-Institut für Aeronomie, Katlenburg-Lindau, Germany.
[6]Department of Physics, University of Arizona, Tucson.
[7]EOS, University of New Hampshire, Durham.
[8]Institute for Space Physics, Moscow, Russia.
[9]Jet Propulsion Laboratory, Pasadena, California.

Paper number 97JA02770.
0148-0227/98/97JA-02770$09.00

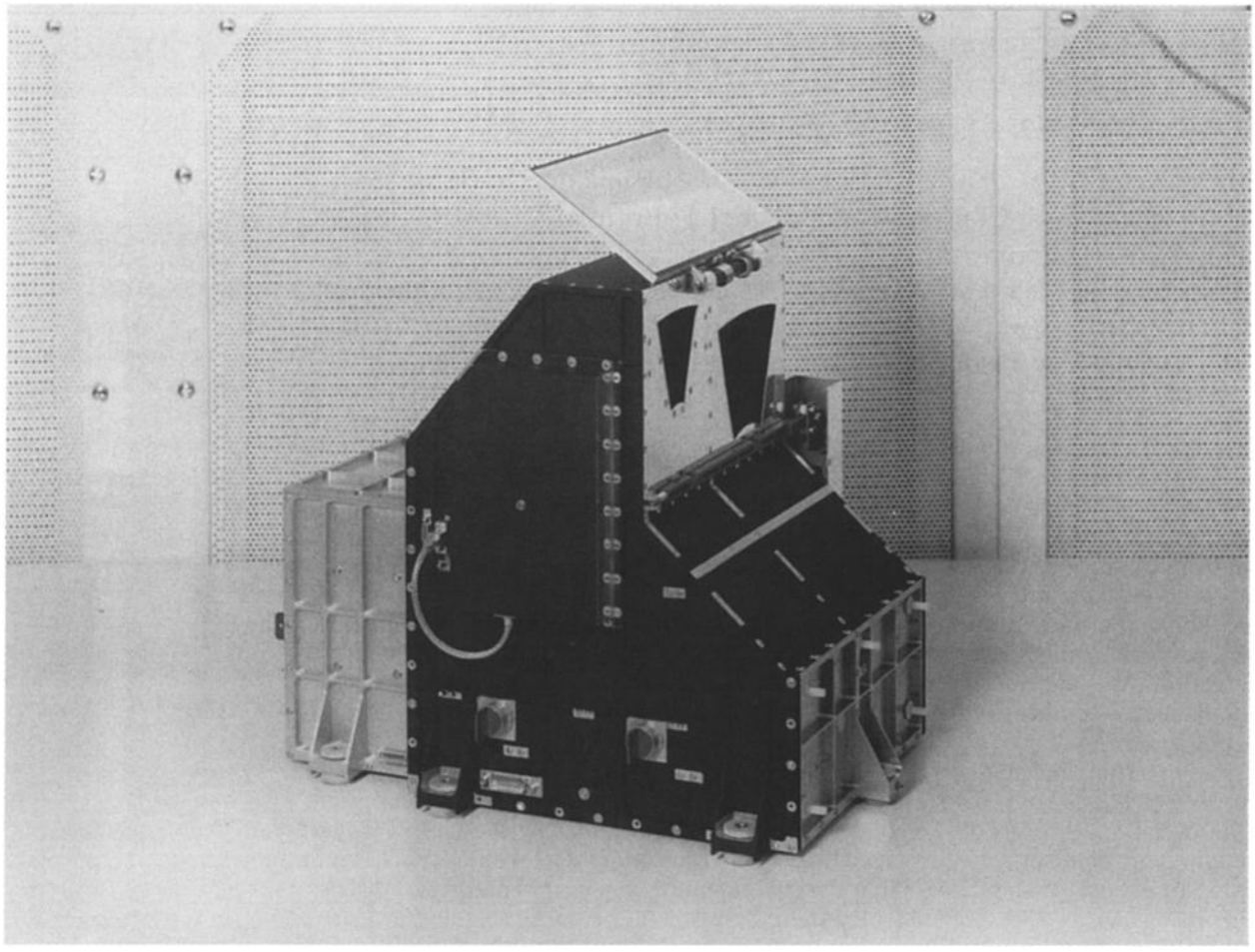

Figure 1. The MTOF experiment viewed from the proton monitor side, showing the wedge-shaped entrance apertures for the (right) main sensor and the (left) proton monitor.

limits the accuracy of derived solar wind parameters. The original SOHO strawman payload included a traditional solar wind plasma experiment and magnetometer that were not able to be accommodated in the final instrument payload selection [*Ness and Smith*, 1988; *Kivelson and Russell*, 1988]. Consequently, the proton monitor became the only SOHO sensor capable of determining the in situ solar wind proton speed, density or temperature. In order to partially recoup additional solar wind plasma information, an enhancement allowing the measurement of solar wind flow direction (in the plane out of the ecliptic) was subsequently approved by the project and added to the proton monitor design. The solar wind speed derived from the proton monitor is contributed to the International Solar Terrestrial Physics (ISTP) Program's "key parameters" database.

The proton monitor has the following science objectives: to provide the solar wind speed and temperature values that are necessary inputs for the efficiency function for the main MTOF sensor; to identify different solar wind flow types; to map the solar wind back to the longitude of its origin above the solar surface; and to provide near-real time solar wind data to the space physics community.

In this paper we present a description of the SOHO proton monitor sensor, our analysis techniques, and some initial flight observations.

2. Instrumentation

The Mass Time-of-Flight (MTOF) experiment of the CELIAS investigation [*Hovestadt et al.*, 1995] contains two sensors. The MTOF/Main is the primary unit, providing solar wind elemental and isotopic abundance measurements. The MTOF/proton monitor is a small auxiliary unit designed to measure the solar wind proton parameters, including speed and direction. Both units are housed within a common structure (see Figure 1), which also contains the low voltage power converter, the high-voltage power supplies, the analog electronics, and the digital electronics. The smaller, leftmost, wedge-shaped black aperture in Figure 1 is the entrance to the proton monitor. (The larger wedge-shaped region is the opening to the main sensor.)

The MTOF proton monitor is a new type of solar wind energy per charge (E/Q) analyzer designed and fabricated by the University of Maryland. It consists of an electrostatic E/Q analyzer similar in form and function to the deflection system used in the MTOF/Main, and a microchannel plate (MCP) detector with a two-dimensional position sensing anode. The PM accepts ions from 0.3 to 6 keV/e with a minimum two-dimensional angular acceptance of $\pm 15°$ and a geometry factor of 1×10^{-4} cm^2. The large angular acceptance is required since the SOHO spacecraft is three-axis stabilized.

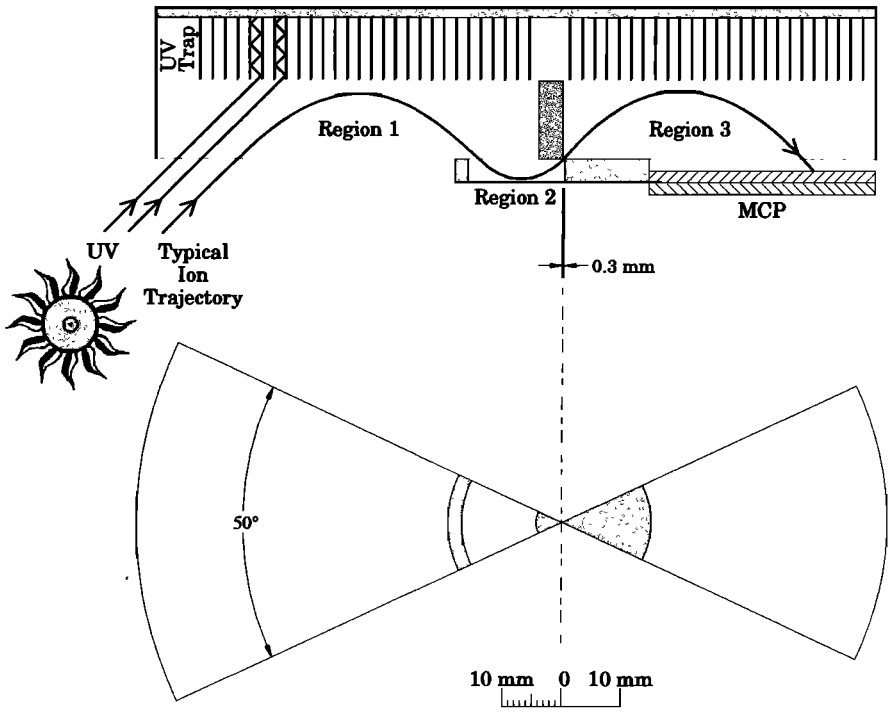

Figure 2. Schematic of the proton monitor showing the locations of the three 50° wedge-shaped deflection regions, the 0.3-mm-diameter pinhole between regions two and three, and the microchannel plate detector.

As illustrated in Figure 2, the E/Q analyzer consists of three 50° wedge-shaped parallel plate deflection regions. Each region is framed by Mecor walls with three linearly spaced thin gold-plated field control electrodes embedded in them. The front of each region through which particles pass is defined by a grid etched in a thin sheet of gold-plated Be-Cu. The back of regions 1 and 3 is open to a simple integrated aluminum UV trap. Voltage is applied in four linear increments from 0 V on the grid to the appropriate positive voltages on the field control electrodes, and the highest voltage ($\leq$4 kV) at the back of each region. The UV trap consists of a series of parallel thin (0.12 mm) flat metal fins (separated by 2 mm with a depth of 10 mm) oriented at an angle of 45 deg to the nominal Sun-spacecraft line. The fins at the back of region 1 are coated with black Ni-Cr. This coating was chosen because of its light absorption properties, excellent electrical conductivity, and relative lack of contamination potential. Incoming photons that are specularly reflected must make at least 4 bounces before reaching the back of the UV trap. Several more bounces are required before the photon could enter region 2, which has a black Ni-Cr coating on its ceiling, and finally region 3 (which also has the aluminum fins, but no coating due to the proximity of the MCP). The three regions are cylindrically symmetric about a 0.3-mm-diameter hole in the Be-Cu sheet between region 2 and region 3 (see Figure 2). The in-flight performance of the PM UV-trapping technique has been excellent. There is no measurable count rate attributable to UV, and after 20 months of exposure there is no evidence of degradation of the coatings.

Figure 3 (top) shows the entrance to region 1 (left), the back of region 2 (middle), and the back of the MCP (right). In Figure 3 (bottom) the MCP has been removed, exposing the exit grid for region 3 and the uncoated aluminum fins at the back of region 3. The MCP detector used in the PM is a custom wedge-shaped Chevron™ design manufactured by Galileo Electro-Optics Corp. The Mecor MCP stack hardware separates the two plates (each 1 mm thick with 40:1 length/diameter ratio) by 0.25 mm. The front of the input plate is negatively biased and the anode is held at ground. In flight, the bias voltage across each plate is 950 V, the voltage across the gap separating the two plates is +40 V, and the anode is at +70 V with respect to the back of the output plate.

Figure 4 shows the cylindrically symmetric two-dimensional ($\mathbf{R}$, θ) position sensing anode, located 1 cm behind the output of the MCP. The anode uses a "sickle/ring" pattern [*Knibbeler et al.*, 1987], with gold-plated copper elements etched on a ceramic substrate. Sickle-shaped elements with width varying linearly with angle provide angular position information. Radial position information is obtained from ring-shaped elements that change width linearly with radial distance from the apex of the anode pattern. A normalization element fills the gaps between the sickle and ring elements. Pulse height information from the three elements is used to calculate the radius and angle position using the following equations: $\mathbf{R}$ = ring / (ring + sickle + norm), θ = sickle / (ring + sickle + norm). The energy per charge (and hence speed) of the incident ions is determined from the $\mathbf{R}$ (radial) position information, while the θ position signal allows the determination of the solar wind flow angle in the plane perpendicular to the ecliptic plane.

The MTOF/PM data accumulation is organized within a commandable six-step deflection plate voltage sequence (5 s/step), thereby acquiring an entire E/Q spectrum every 30 s.

3. Analysis Technique

Our routine analysis to date has not included the radius position information that is available within each voltage step. This information, under conditions of low kinetic temperature, allows the derivation of the density of He^{++} in the solar wind.

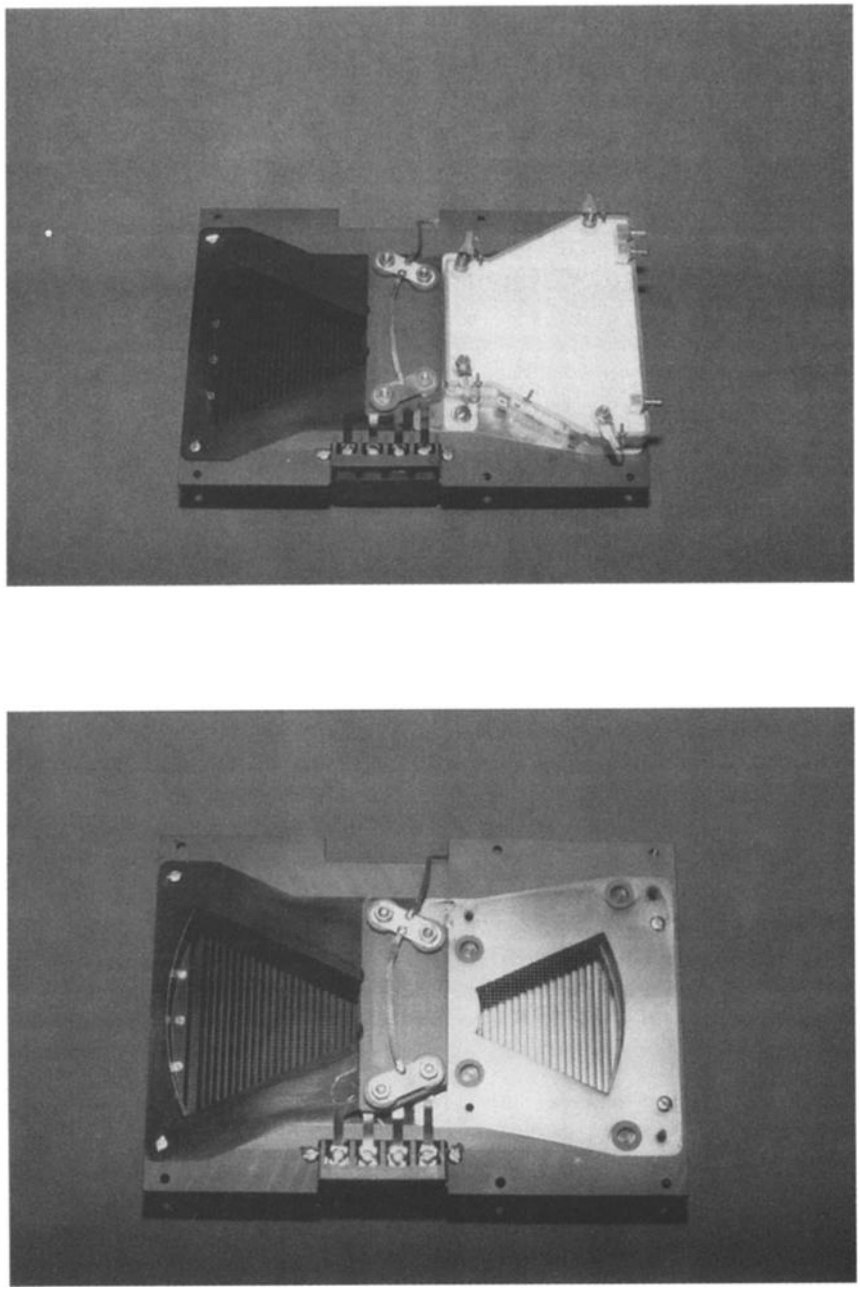

Figure 3. (top) The front of the proton monitor with the microchannel plate detector installed. (bottom) Same except the microchannel plate detector has been removed; the UV traps behind regions one and three are visible through the etched grids.

The θ position information is being used to determine the solar wind H^+ flow direction. The H^+ bulk speed, thermal speed, and density are derived from the sets of six rates (one for each voltage step of the PM deflection system) that are obtained every 30 s. In the nominal stepping sequence, the voltage steps are spaced logarithmically (60% step size) from 0.3 to 3 kV. At a given voltage step the energy per charge dynamic range is slightly more than a factor of 2. Two independent methods were used to derive the solar wind parameters: a fitting technique and a moment-calculating technique.

In the fitting method, solar wind parameters are derived by comparing the six measured rates with those resulting from a simulation program. The simulation assumes that solar wind protons may be represented by a convected Maxwellian distribution, characterized by a bulk speed and temperature. An alpha particle fraction of 4% is assumed. A heavy ion component with density of 0.025 of the He^{++} density is assumed at a mass/charge value of 2.7. The alphas and heavy ions are assumed to have the same temperature per mass as the protons. A fixed solar wind proton density (10 cm^{-3}) is used in an analytic integration of the convected Maxwellians over the bandwidth of the deflection system to derive the expected absolute counting rates.

The simulation assumes the following values of the two variables: The solar wind speed is allowed to vary from 235 to 1042 km/s in 250 logarithmic steps of 0.6%; the Mach number (the ratio of bulk speed to the most probable thermal speed) is varied from 3.5 to 34.5 in 25 logarithmic steps of 10%. For each

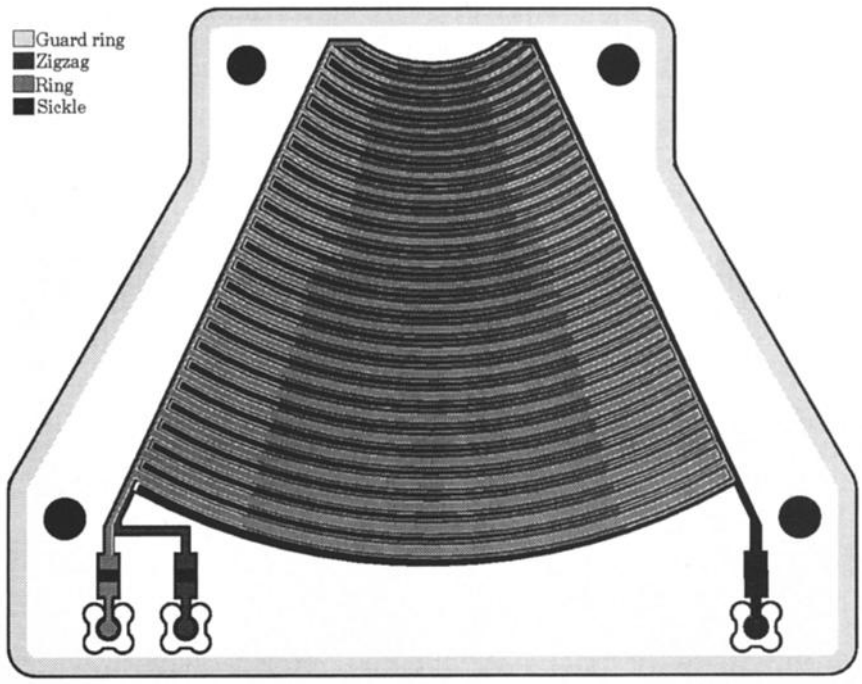

Figure 4. The two-dimensional cylindrically symmetric position sensing anode used in the proton monitor.

combination of the two variables a set of six rates is derived from the simulation. A total of 250 × 25 = 6250 "sextuplets" is thereby created. Each of the sextuplets is then compared with a measured set of six rates. For each comparison the sum of the six simulated rates is normalized to equal the sum of the six measured rates; the normalization factor is then used to derive the solar wind density. Finally, a goodness of fit parameter is used to select the best set of simulation parameters for a given set of six measured rates.

The second method uses simple numerical integration to calculate the moments of the distribution represented by the six rates. The density is derived from the weighted sum, the speed from the first moment, and the thermal speed from the square root of the second moment.

The θ position signal (described in the Instrumentation section) is used by the Data Processing Unit to construct a set of 20 theta bins. The number of counts in each of these 20 angle bins (summed across all six voltage steps) are used to calculate an average bin number, from which the out-of-ecliptic angle is derived.

4. Comparison With the Wind/SWE Instrument

We have compared the PM solar wind parameters derived from both approaches with those derived from the SWE instrument on the Wind spacecraft (courtesy K. W. Ogilvie and A. J. Lazarus). The time period analyzed was January 20, 1996, to January 31, 1997. The SWE data consisted of key parameter data files (92-s averages). Time periods when Wind had an X_{GSE} position of $<50\ R_E$ were deleted (to minimize the influence of the Earth's bow shock).

In order to partially compensate for the solar wind travel time between SOHO and Wind, the SWE data were shifted by a (constant) time, calculated as follows: The difference between the median X_{GSE} coordinates for Wind and SOHO (116 and 220 R_E, respectively) was divided by the average observed solar wind speed (420 km/s), yielding a median time delay of 26 min. Five-minute PM parameters were averaged over fixed 2-hour intervals. The SWE parameters, after time shifting, were then averaged over the same 2-hour intervals. It was required that both instruments have at least 80% data coverage for a 2-hour interval to be accepted. Of the 4527 possible intervals, 4399 were accepted for SOHO and 3583 for Wind. The combined data set consisted of 3479 simultaneous 2-hour data points.

The SWE data set was used to refine the PM solar wind parameters derived from both the fitting and moment techniques. It was found that the moment technique produced higher correlation coefficients when compared to SWE parameters for bulk speed and thermal speed, while the fitting technique produced a higher correlation coefficient for density. The two techniques were then combined as follows. For the bulk speed, the ratio of PM (moment) and SWE values was correlated with the ratio of bulk speeds derived from the two techniques, and a correction function thereby obtained; the same was done for the thermal speed. For the density, the ratio of PM (fit technique) and SWE values was correlated with the density ratio derived from the two techniques to derive the correction function. Unless otherwise indicated, all results from the PM quoted below were obtained using this combined technique.

Figure 5 displays the frequency distribution of the ratio of the proton bulk speeds observed by PM and SWE. The standard deviations of the distribution of the ratios of solar wind parameters derived by the PM and SWE instruments are 2.1% for the bulk speeds, 17% for the densities, and 16% for the thermal speeds. Some of the spread in these distributions is undoubtedly real, reflecting different solar wind conditions at the locations of the two spacecraft that are sometimes separated by more than 100 R_E in the Y_{GSE} direction. The correlation coefficients for the solar wind parameters from the two

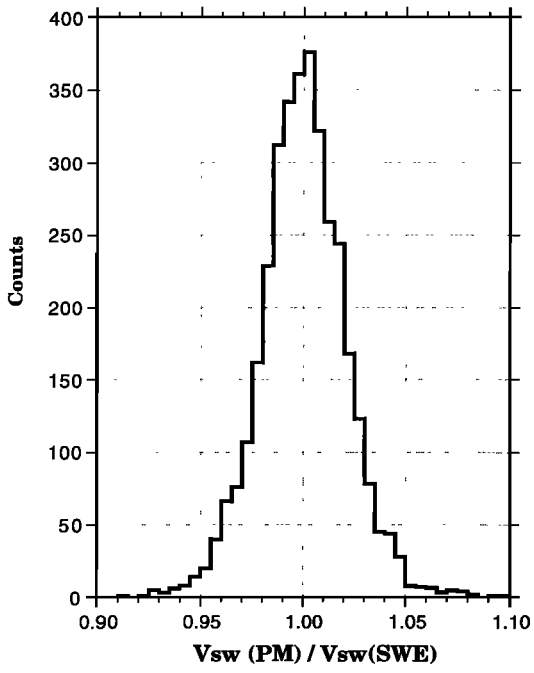

Figure 5. Frequency distribution of the ratios of proton bulk speeds observed by the proton monitor (PM) on the SOHO spacecraft and SWE on the Wind spacecraft.

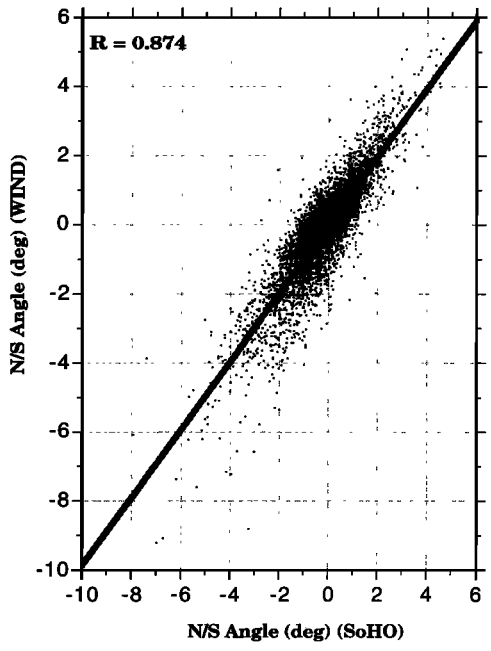

Figure 6. Scatterplot of the solar wind flow angles (positive angles indicate flow from the south, negative angles indicate flow from the north) observed by SOHO/PM and Wind/SWE. The line represents a least squares fit, correlation coefficient $R = 0.874$.

spacecraft are given in Table 1. A scatterplot of the solar wind flow angle (in the plane perpendicular to the ecliptic) observed simultaneously by the PM and SWE instruments is presented in Figure 6.

5. Observations

In this section we present a variety of in-flight results obtained from the proton monitor. Table 2 lists the average values of a number of standard solar wind proton parameters obtained from the data set discussed above (i.e., 2-hour averages, approximately 1-year data coverage). The standard deviation of the distribution is also listed for each parameter. It should be noted that the time period of these observations is basically during solar minimum conditions.

Figure 7 is a scatterplot of the solar wind proton density and bulk speed, obtained over the same ~1-year time period. A least squares power law fit to this data set has a slope of approximately −1.9; i.e., $N_p \propto V_{sw}^{-1.9}$. Hence the number flux ($= N_p V_{sw}$) varies as $V_{sw}^{-0.9}$, and the momentum flux ($= N_p m_p V_{sw}^2$, where m_p is the proton mass) is nearly independent of speed, varying as $V_{sw}^{+0.1}$. The kinetic energy flux ($= 0.5 N_p m_p V_{sw}^3$) increases with speed, varying as $V_{sw}^{+1.1}$.

Figures 8 and 9 present PM measurements of probable interplanetary shock waves observed in early 1997, using the highest available time resolution (30 s). Preliminary evidence from other SOHO experiments suggests that both of these shocks may be associated with coronal mass ejections (CMEs). About 18 hours after the February 9, 1997, shock passage, the PM observed an unusual density depletion. Figure 10 presents the PM density measurements derived separately using the fitting and moment techniques discussed in section 3. The two techniques are in good agreement during this time period. The density remained below 1 cm^{-3} for ~5 hours, attaining a minimum value of ~0.2 cm^{-3}. These are the lowest densities observed by the PM in its 20 months of operation. The solar wind speed during this period varied from ~420 to 470 km/s. Since SOHO has no magnetometer, we have used magnetic field data from the MFI instrument (courtesy R. P. Lepping) on the Wind spacecraft to estimate the local Alfven speed. At this time the GSE separation of the two spacecraft was ~1, 74, and 27 R_E in X, Y, and Z, respectively. The magnetic field magnitude during the 5 hours of interest was quite steady with an average value of 8.5 nT. The peak calculated Alfven speed

Table 1. Correlation Coefficients for Solar Wind Parameters Derived From the SOHO and WIND Spacecraft

H^+ Parameter	Correlation Coefficient (SOHO/PM versus Wind/SWE)
Bulk speed	0.993
Density	0.892
Thermal speed	0.899
Angle out of ecliptic	0.874

Table 2. Solar Wind Averages From SOHO/PM (January 20, 1996, to January 31, 1997)

H^+ Parameter	Mean	Standard Deviation
Bulk speed, km/s	421	76
Density, cm^{-3}	8.1	4.3
Thermal speed, km/s	35	11
Sonic Mach number	12.5	2.0
Number flux, 10^8 cm^{-2} s^{-1}	3.2	1.4
Momentum flux, 10^{-8} dynes cm^{-2}	2.2	0.9
Kinetic energy flux erg cm^{-2} s^{-1}	0.46	0.21
N/S angle, deg	−0.2	1.5

was ~420 km/s, somewhat less than the solar wind speed of 460 km/s at that time. The solar wind Alfven Mach number was thus quite low (about 1.1), but the solar wind was still super-Alfvenic.

The very low solar wind ram pressure at this time would be expected to cause the Earth's magnetopause and bow shock to expand much beyond their nominal locations. A possible consequence of this magnetospheric expansion is presented in Figure 11, which displays the flux of electrons with energies above 2 MeV observed by the geosynchronous GOES 9 spacecraft during February 9–10, 1997. The shaded region represents the time period (shifted by 1 hour to account for the solar wind propagation time from SOHO to the Earth) when the observed PM density was below 1 cm^{-3}. A large increase in the electron flux appears to be initiated by the very low solar wind density. The peak flux attained on February 10 is unusually high; we have searched the previous 12 months of GOES data and found this to be the highest flux observed.

6. Discussion

We have demonstrated that the proton monitor generates reasonably accurate solar wind proton parameters (see Table 1). The PM can identify interplanetary shocks (Figures 8 and 9) as well as very low density regions (Figure 10). Using the existing 1-year PM database we have found that the solar wind proton momentum flux is very nearly independent of speed. The near invariance of the momentum flux has been emphasized by *Schwenn* [1990] based on analysis of Helios solar wind data from December 1974 to December 1976 (a period of low solar activity, as is the data set reported in this paper). Their average observed momentum flux (extrapolated from the Helios position to 1 AU) was 2.15 × 10^{-8} dynes/cm^2 (equivalently, 2.15 nPa), essentially the same as our observed value (2.2 × 10^{-8} dynes/cm^2, see Table 2). *Phillips et al.* [1996] presented an analysis of Ulysses solar wind proton data from September 1994 to June 1995, during which time the spacecraft traversed heliographic latitudes from −80.2° to +64.9°. They found that the proton mass flux (equivalently proton number flux), scaled to 1 AU, was nearly constant with latitude, while the momentum flux was highest at high latitudes. This variable momentum flux (which is effectively the dynamic pressure exerted by the solar wind) led *Phillips et al.* [1996] to suggest a latitudinal asymmetry in the heliopause cross section. Since the solar wind speed is highly correlated with latitude, it is likely that for their data set the momentum flux also varies with speed, in contrast to the in-ecliptic results presented by *Schwenn* [1990] and in this work.

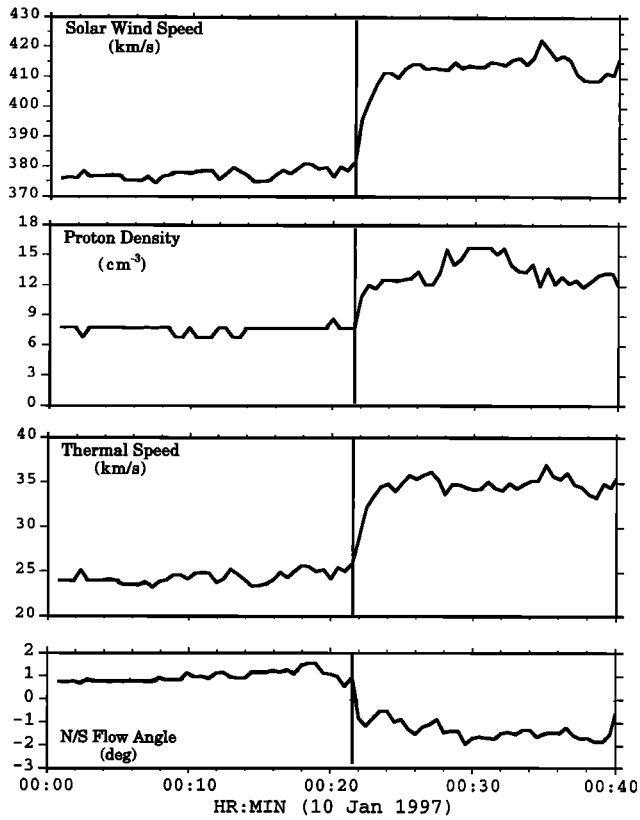

Figure 8. PM observations of a probable interplanetary shock, 30-s averages.

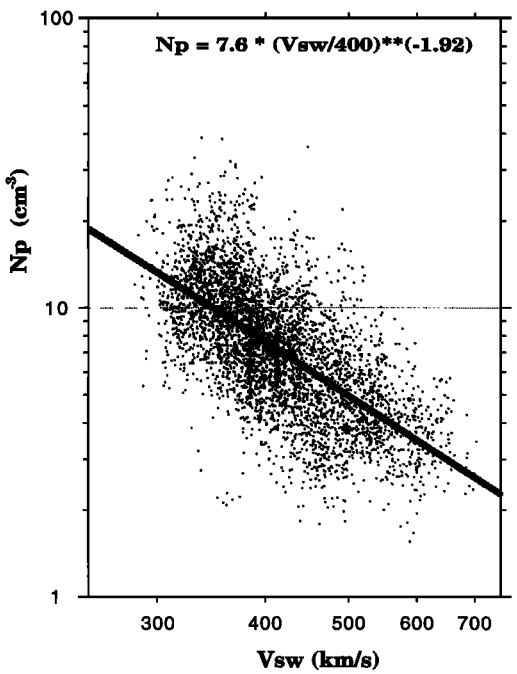

Figure 7. Scatterplot of the proton density versus the proton bulk speed observed by the PM (2-hour averages, approximately 1-year data coverage). The least squares line is based on a power law fit, with slope −1.92 and correlation coefficient 0.58.

The very low solar wind density time period observed by SOHO (Figure 10) appears to be associated with a large increase in the flux of magnetospheric electrons with energies above 2 MeV observed by GOES 9 at geosynchronous altitudes (Figure 11). This flux increase (the largest in at least a year) may possibly have been caused by a nonadiabatic redistribution of inner radiation belt electrons as the magnetosphere expanded in response to the very low solar wind ram pressure. Somewhat ironically, it may be that the strongest doses of relativistic electrons at geosynchronous altitudes may be the result of the very weakest solar wind.

One may ask how often the solar wind contains such very large density depletions. Recently, *Riley et al.* [1998] reported a unique "density hole" in their Ulysses spacecraft data set. The event, lasting ~3.5 hours, was observed at 3.7 AU and 38.5°

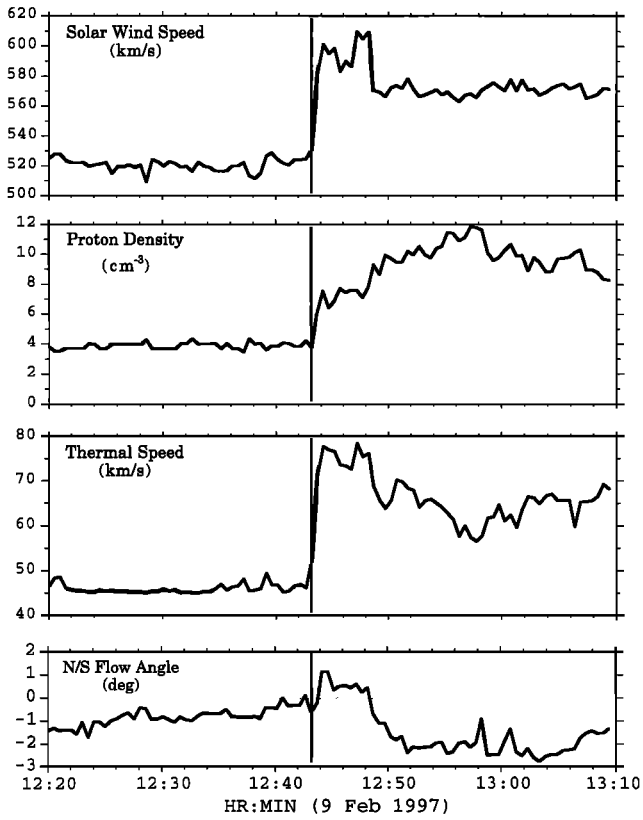

Figure 9. PM observations of another probable interplanetary shock, 30-s averages.

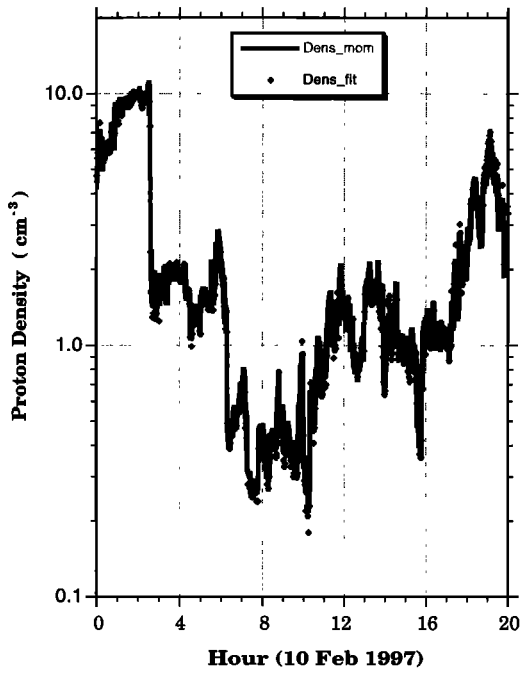

Figure 10. PM density measurements (2-min averages) during an unusually low density time period. The gray solid line represents the density as derived from the moment technique, while the points represent the density obtained from the fitting technique.

heliographic latitude in the otherwise uniform fast solar wind. *Gosling et al.* [1982] presented ISEE 3 observations of several large density depletions. During portions of an ~5-hour long event on November 22, 1979, these authors report that the solar wind was sub-Alfvenic. The event was not associated with a shock or with a rarefaction region that could be dynamically produced in a region of declining solar wind speed. *Gosling et al.* [1982] also report a pair of density depletion events (July 4 and 31, 1979) that may have been caused by a quasi-stationary corotating structure.

In order to explore the systematics of large density depletions we have examined the NSSDC OMNIWeb database, consisting of 1-hour averages of solar wind parameters. We considered the period from January 1, 1974, to January 1, 1984 (after this time the OMNIWeb data set may have artificially suppressed very low densities (A. J. Lazarus, private communication, 1997)). The average data coverage was ~70% during this 10-year interval. Large density depletions were identified with those hourly intervals with an average proton density less than or equal to 0.5 cm^{-3}. A total of 72 hourly intervals were found (out of a total of ~60,000 hours of data coverage). We further defined "events" as contiguous or nearly contiguous groupings of these 72 intervals (intervals separated by less than 30 hours were considered part of the same event). This definition resulted in nine events over the 10-year period. The average event duration, 8 hours, corresponds to a spatial scale of ~0.1 AU. The shortest event consisted of a single hourly average (June 6, 1979) and the longest consisted of 20 hourly averages (July 31 to August 1, 1979). Of the nine events, four occurred in 1979. The three events reported by *Gosling et al.* [1982] were all identified with this analysis technique. In addition to the pair of density depletion events (July 4 and 31, 1979) identified by *Gosling et al.* [1982] as possibly being corotating, the OMNIWeb analysis identified an event on June 6, 1979, that is consistent with a third rotation; however, none of

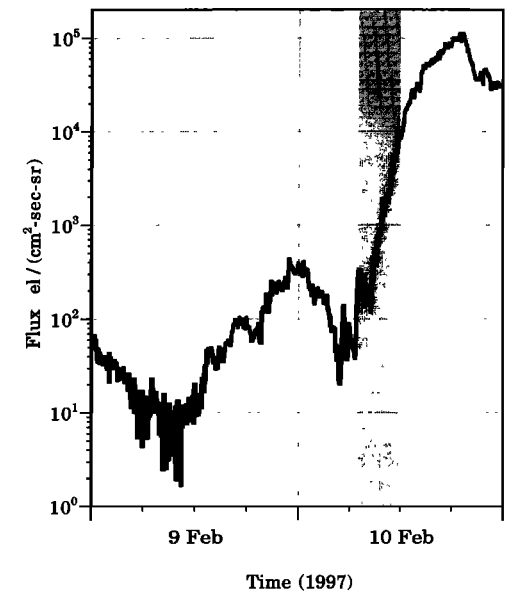

Figure 11. Energetic electron flux observed on the geosynchronous spacecraft GOES 9. The shaded region represents the time interval (delayed by 1 hour to account for the solar wind propagation time from SOHO to the Earth) when the PM density was below 1 cm^{-3}.

the other nine events were corotating. The start of one of the events (1800 UT on September 29, 1978) occurred ~16 hours after the passage of a CME-associated interplanetary shock (the shock and CME were discussed by *Ipavich et al.* [1986] and *Galvin et al.* [1987]). The event on February 10, 1997, reported in the present work began ~18 hours after a CME-associated shock. Using the above event definition, the SOHO/PM data set produces one event in 20 months of data coverage; combined with the OMNIWeb analysis this results in an average frequency of about one large density depletion per year in the solar wind observed near Earth. The origin of these events remains unknown; of 10 total events, 3 appear to be corotating, and at least 2 are probably CME related.

The excellent and rapid data availability from SOHO has allowed us to construct a page on the World Wide Web that presents proton monitor results on a near real time basis. The data are obtained by automatic electronic transfer from the Experimenters' Operations Facility at Goddard Space Flight Center to the University of Maryland. When files are received (typically every 30 min), several automated batch processes analyze and plot the data and dynamically update the Web page. The data on the Web page are typically between a few minutes and a few hours old. In addition to the most recent data, a catalog of 27-day (Carrington rotation) plots are available from the Web page. The proton monitor data set is currently available on the World Wide Web at http://umtof.umd.edu/pm.

Acknowledgments. We are very grateful to K. W. Ogilvie and A. J. Lazarus for the use of the Wind/SWE solar wind data set. We also thank R. P. Lepping for Wind/MFI magnetic field data and acknowledge the use of the OMNIWeb database from the NSSDC, and the GOES data set from the U.S. Dept. of Commerce, NOAA, Space Environment Center. Finally, we thank the many individuals at the University of Maryland and the other CELIAS Institutions who contributed to the success of this experiment. This research was supported by NASA grant NAG5-2754, the Swiss National Science Foundation, and by DARA, Germany under contracts 50 OC 89056 and 50 OC 96059.

The Editor thanks J. L. Burch and another referee for their assistance in evaluating this paper.

References

Domingo, V., B. Fleck, and A. I. Poland, The SOHO mission: An overview, *Sol. Phys.*, *162*, 1, 1995.

Galvin, A. B., F. M. Ipavich, G. Gloeckler, D. Hovestadt, S. J. Bame, B. Klecker, M. Scholer, and B. T. Tsurutani, Solar wind iron charge states preceding a driver plasma, *J. Geophys. Res.*, *92*, 12069, 1987.

Gosling, J. T., J. R. Asbridge, S. J. Bame, W. C. Feldman, R. D. Zwickl, G. Paschmann, N. Sckopke, and C. T. Russell, A sub-Alfvenic solar wind: Interplanetary and magnetosheath observations, *J. Geophys. Res.*, *87*, 239, 1982.

Hovestadt, D., et al., CELIAS - charge, element, and isotope analysis system for SOHO, *Sol. Phys.*, *162*, 441, 1995.

Ipavich, F. M., A. B. Galvin, G. Gloeckler, D. Hovestadt, S. J. Bame, B. Klecker, M. Scholer, L. A. Fisk, and C. Y. Fan, Solar wind Fe and CNO measurements in high speed flow, *J. Geophys. Res.*, *91*, 4133, 1986.

Kivelson, M. G., and C. T. Russell, Forum: SOHO: An unfortunate omission, *Eos Trans. AGU*, *69*, 636, 1988.

Knibbeler, C. L. C. M., G. J. A. Hellings, H. J. Maaskamp, H. Ottevanger, and H. H. Brongersma, Novel two-dimensional position-sensitive detection system, *Rev. Sci. Instrum.*, *58*(1), 125, 1987.

Ness, N. F., and E. J. Smith, Forum: SOHO? No, SOSO, *Eos Trans. AGU*, *69*, 636, 1988.

Phillips, J. L., S. J. Bame, W. C. Feldman, J. T. Gosling, and D. J. McComas, Ulysses solar wind plasma observations from peak southerly latitude through perihelion and beyond, in *Solar Wind Eight*, edited by D. Winterhalter et al., *AIP Conf. Proc. 382*, p. 416, AIP Press, Woodbury, N. Y., 1996.

Riley, P., J. T. Gosling, D. J. McComas, and R. D. Forsyth, Ulysses observations of a "density hole" in the high-speed solar wind, *J. Geophys. Res.*, in press, 1998.

Schwenn, R., Large scale phenomena, in *Physics of the Inner Heliosphere*, edited by R. Schwenn and E. Marsch, pp. 99–181, Springer-Verlag, New York, 1990.

W. I. Axford, H. Grünwaldt, M. Hilchenbach, E. Marsch, and B. Wilken, Max-Planck-Institut für Aeronomie, D-37189 Katlenburg-Lindau, Germany. (e-mail: gruenwaldt@linax1.dnet.gwdg.de)

H. Balsiger, P. Bochsler, J. Geiss, S. Hefti, R. Kallenbach, and P. Wurz, Physikalisches Institut der Universität, CH-3012 Bern, Switzerland. (e-mail: bochsler@soho.unibe.ch)

A. Bürgi, D. Hovestadt, B. Klecker, and M. Scholer, Max-Planck-Institut für extraterrestriche Physik, D-85470 Garching, Germany. (e-mail: bek@mpens.mpe-garching.mpg.de)

M. A. Coplan, A. B. Galvin, G. Gloeckler, F. M. Ipavich, S. E. Lasley, and J. A. Paquette, Department of Physics, University of Maryland, College Park, MD 20742. (e-mail: ipavich@umtof.umd.edu)

F. Gliem and K.-U. Reiche, Institut für Datenverarbeitungsanlagen, Technische Universität, D-38023 Braunschweig, Germany. (e-mail: gliem@ida.ing.tu-bs.de)

K. C. Hsieh, Department of Physics, University of Arizona, Tucson, AZ 85721. (e-mail: hsieh@soliton.physics.arizona.edu)

M. A. Lee and E. Möbius, EOS, University of New Hampshire, Durham, NH 03824. (e-mail: moebius@rotor.sr.unh.edu)

G. G. Managadze and M. I. Verigin, Institute for Space Physics, Moscow, Russia. (e-mail: gmanagad@esoc.bitnet)

M. Neugebauer, Jet Propulsion Laboratory, Pasadena, CA 91103. (e-mail: mneugeb@jplsp.jpl.nasa.gov)

(Received April 1, 1997; revised September 17, 1997;
accepted September 25, 1997.)